International Journal of Modern Physics E

Quantum fluctuations and stability of tetrahedral deformations in atomic nuclei.

K. Zberecki, P. Magierski
Faculty of Physics, Warsaw University of Technology, ul. Koszykowa 75, 00-662 Warsaw, Poland

P.-H. Heenen
Service de Physique Nucléaire Théorique, U.L.B - C.P. 229, B 1050 Brussels, Belgium

N. Schunck
Institute of Theoretical Physics, ul. Hoza 69, 00-631 Warsaw, Poland

University of Surrey, Guildford GU2 7XH, UK

Received (received date)
Revised (revised date)

The possible existence of stable axial octupole and tetrahedral deformations is investigated in ^{80}Zr and ^{98}Zr. HFBCS calculations with parity projection have been performed for various parametrizations of the Skyrme energy functional. The correlation and excitation energies of negative parity states associated with shape fluctuations have been obtained using the generator coordinate method (GCM). The results indicate that in these nuclei both the axial octupole and tetrahedral deformations are of dynamic character and possess similar characteristics. Various Skyrme forces give consistent results as a function of these two octupole degrees of freedom both at the mean-field level as well as for configuration mixing calculations.

1. Introduction

It has been recently conjectured that many nuclei throughout the periodic table possess a tetrahedral deformation in their ground- or low-lying isomeric state. This type of deformation is realized mainly through the non-zero intrinsic octupole moment $Q_{32} \propto r^3(Y_{32} + Y_{3-2})$ accompanied by vanishing quadrupole deformation. The first study pointing at the importance of the tetrahedral degree of freedom in many-fermion systems has been reported in Ref. [1]. Recently more realistic approaches based on the microscopic-macroscopic model with Woods-Saxon Hamiltonian revealed that several nuclei may possess stable tetrahedral deformation. These nuclei are believed to form islands on the nuclear chart around "tetrahedral magic" numbers of neutrons and protons: $16, 20, 32, 40, 56-58, 70, 90-94$[2,3,4]. The enhanced susceptibility towards the tetrahedral deformation is associated with the symmetry of pyramid-like shapes. It leads to the appearance of two- and four-fold degeneracies in the single-particle spectrum and consequently generates large shell effects stabilizing this deformed configuration [3,2,4,5].

On the other hand the energy difference between the spherical and tetrahedral configurations is a sensitive function of the pairing strength. Consequently a stable tetrahedral deformation is a result of a delicate balance between shell effects and pairing correlations. Indeed it was shown that for two tetrahedral magic nuclei: ^{80}Zr and ^{98}Zr, the energy difference between spherical and tetrahedral configurations does not exceed 1 MeV. Consequently quantum fluctuations beyond the mean-field play a significant role [6]. Moreover these nuclei also exhibit other types of octupole deformations: the coupling between the neutron $d_{5/2}$ and $h_{11/2}$ orbitals and the proton $p_{3/2}$ and $g_{9/2}$ orbitals leads to both axial and non-axial octupole correlations [7,6]. Moreover octupole deformations are in competition with the quadrupole mode.

In the present article we analyze the influence of various parametrizations of the Skyrme interaction and pairing strengths on the existence of tetrahedral deformation in ^{80}Zr and ^{98}Zr. In the first section the competition between axial octupole and tetrahedral shapes at the mean-field level is discussed. In the next section the nuclear dynamics beyond the mean-field is investigated. This study is directed towards the determination of the correlation energies and excitation energies of negative parity states.

2. Hartree-Fock + BCS approach and the parity projection.

The Hartree-Fock + BCS (HFBCS) method has been applied to obtain the energy of a nucleus as function of octupole degrees of freedom. The Hartree-Fock equations have been solved on a 3-dimensional mesh in coordinate space. The details of the calculations can be found in Refs. [8,9,6]. The pairing interaction has been treated in the BCS approximation including the Lipkin-Nogami (LN) correction [10]. A zero-range density-dependent pairing interaction has been used:

$$V_{pair} = \frac{1}{2} g_i (1 - P_\sigma) \delta(\mathbf{r} - \mathbf{r}') \left(1 - \frac{\rho(\mathbf{r})}{\rho_0} \right), \tag{1}$$

where $i = n, p$ for neutrons and protons, respectively. As in previous applications, we set $\rho_0 = 0.16\text{fm}^{-3}$. The strength of the pairing force has been adjusted to "experimental" pairing gaps, extracted from the odd-even mass staggering using a three-point filter from Ref. [11].

The behavior of the HFBCS energy as function of the axial octupole and tetrahedral degrees of freedom qualitatively agrees with the results presented in Ref. [12,13,14]. The existence of axial and non-axial octupole minima is a sensitive function of the pairing strength. The minima are not well pronounced and vanish when pairing is increased [6]. However the HFBCS approach does not conserve neither parity nor particle number. Namely, the HFBCS solutions represents a mixture of positive and negative parity states.

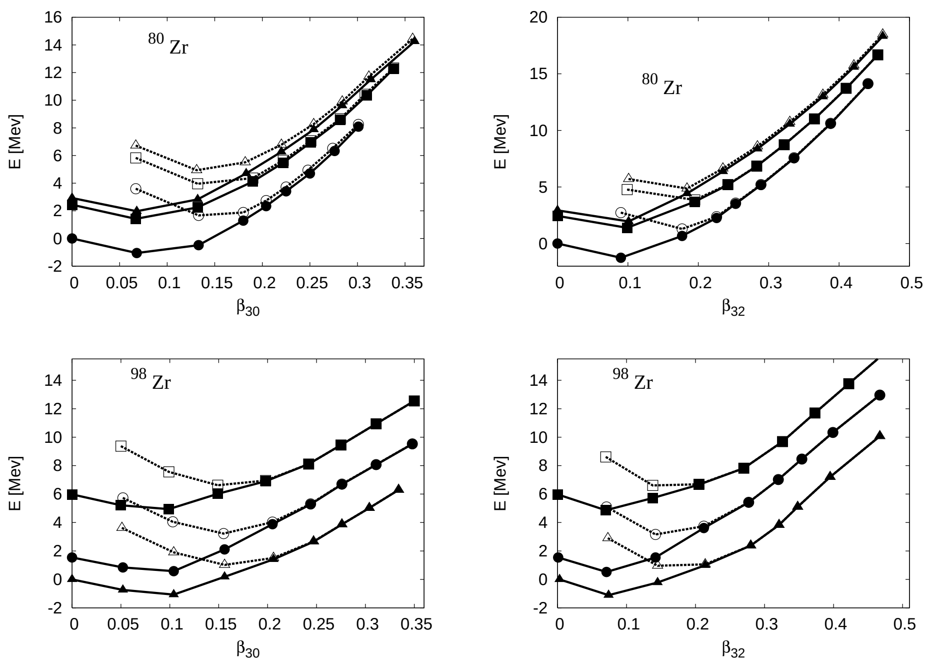

Fig. 1. The parity-projected mean-field energy as function of shape parameters $\beta_{3\mu}$ (see text for definition) is shown for three parametrizations of the Skyrme force. The two figures at the left-hand side show the energy as function of the axial octupole shape parameter β_{30}, whereas the figures at the right-hand side show the energy as function of β_{32}. The solid lines with filled symbols denote positive parity solutions and the dotted lines with open symbols denote negative parity solutions. Circles, triangles and squares correspond to the Skyrme parametrization: Sly4, SkM* and SIII, respectively. The energies are shown relative to the lowest energy of the spherical configuration.

The restoration of broken symmetries has been performed through the projection on a definite parity and particle number. The corrected energies for N neutrons, Z protons and both parities are obtained by exact projection:

$$E(N,Z,\beta_{3\mu})_{\pm} = \frac{\langle\phi(\beta_{3\mu})|\hat{H}\hat{P}_{(\pm,N,Z)}|\phi(\beta_{3\mu})\rangle}{\langle\phi(\beta_{3\mu})|\hat{P}_{(\pm,N,Z)}|\phi(\beta_{3\mu})\rangle}, \tag{2}$$

where $|\phi(\beta_{3\mu})\rangle$ are HFBCS wave functions generated with the constraint $\langle\phi(\beta_{3\mu})|\hat{Q}_{3\mu}|\phi(\beta_{3\mu})\rangle = C_\mu\beta_{3\mu}$. The shape parameters $\beta_{3\mu}$ are related to the octupole moments through the relation: $\beta_{30} = \langle Q_{30}\rangle/C_0$, $\beta_{32} = \langle Q_{32}\rangle/C_2$, where $C_0 = \dfrac{3}{4\pi}A^2 r_0^3, C_2 = C_0/\sqrt{2}$ with $r_0 = 1.2fm$. The operator $\hat{P}_{(\pm,N,Z)}$ is the product of operators projecting on $\pi = \pm 1$ parity and on N neutrons and Z protons.

The parity-projected energies for three parametrizations of the Skyrme force are shown in the Fig. 1. One may notice that all forces give qualitatively the same dependence (apart from a trivial energy shift) as function of the axial octupole

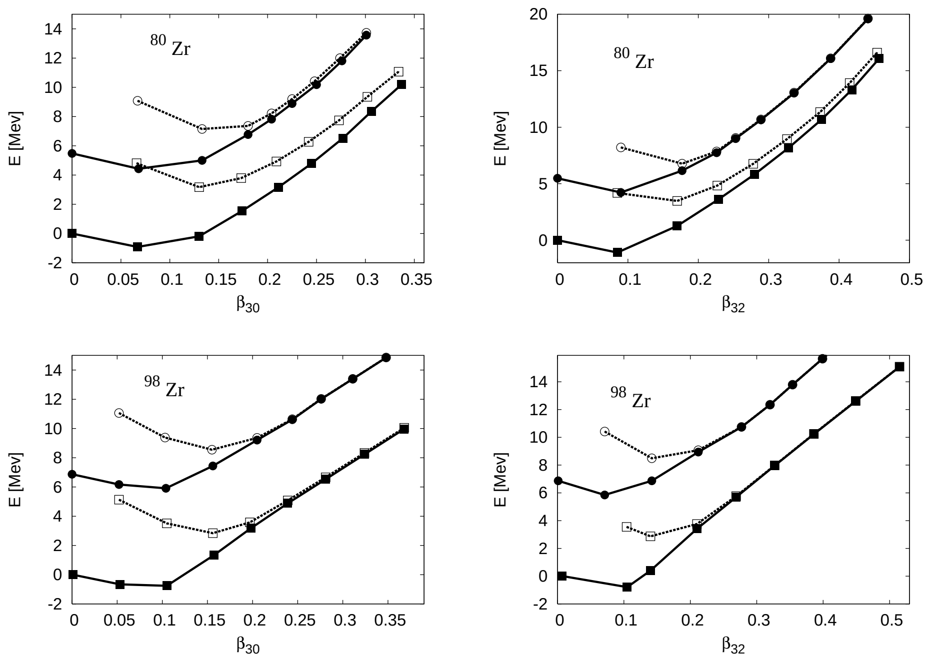

Fig. 2. The parity projected mean-field energy as function of shape parameters $\beta_{3\mu}$ obtained using the Sly4 force. Two values of the pairing strength have been used: reproducing the experimental gaps (circles) and with pairing gaps increased by a factor 2 (squares). The solid (dotted) lines with filled (open) symbols denote positive (negative) parity solutions.

and tetrahedral degree of freedom. As usual after parity restoration [15] the energy minima for positive parity states are shifted towards smaller octupole deformations compared to the HFBCS minima, while the negative parity states have larger deformations. For both nuclei the energy minima for positive parity correspond to very similar β_{30} and β_{32} values. For the negative parity curve, β_{32} is systematically larger than β_{30} in the minimum.

It is instructive to investigate the sensitivity of the parity projected solutions to the pairing strength. In the Fig. 2 we have shown the parity projected energies for the SLy4 parametrization of the Skyrme force for normal and increased (twice) strength of pairing correlations. Note that contrary to the behavior of unprojected HFBCS energies, in this case the dependence of the energy as function of octupole degrees of freedom practically remains unchanged. In particular, the position of the energy minima for both negative and positive parity states remains unaltered. Similar results have been obtained for other Skyrme parametrizations.

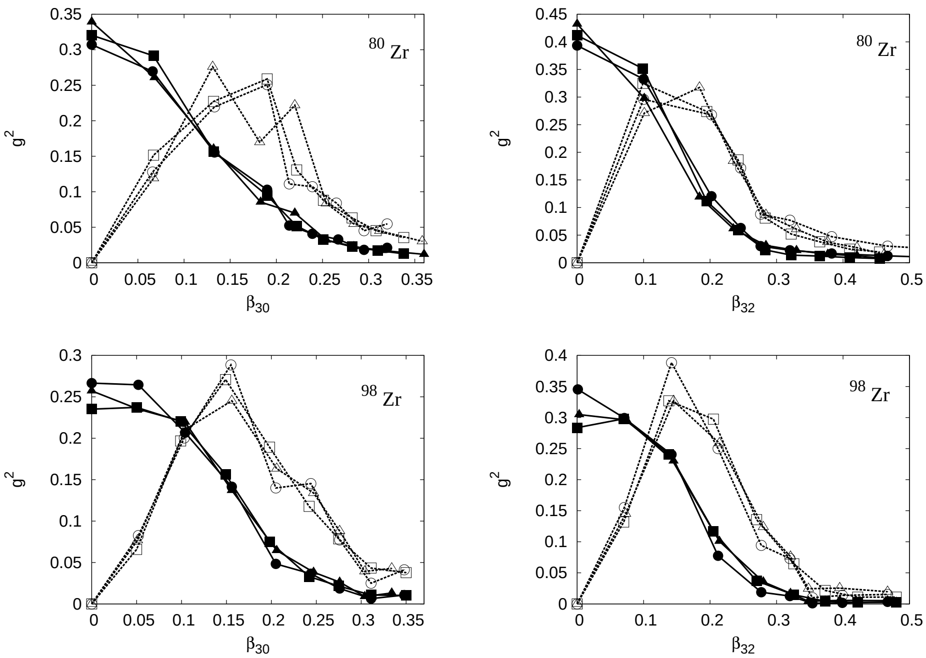

Fig. 3. The square of the modulus of the collective wave function vs. shape parameters $\beta_{3\mu}$ are plotted for three parametrizations of the Skyrme force. The two figures at the left-hand side show the energy as a function of the axial octupole shape parameter β_{30}, whereas the two at the right-hand side show the energy as function of β_{32} (see text). The symbols used for each curve are the same as in Fig. 1.

3. Generator coordinate method.

Mean-field results suggest that shape fluctuations are important in this case. In order to quantify this effect we have applied the generator coordinate method (GCM). It allows to calculate the correlation energies associated with shape fluctuations and to determine the structure of the collective wave functions in terms of the contributing mean-field configurations. Namely, a collective wave function is constructed by mixing the mean-field states corresponding to different values of the octupole moment, after their projection on particle number and parity:

$$|\Psi\rangle = \int f(\beta_{3\mu})\hat{P}_{(\pm,N,Z)}|\phi(\beta_{3\mu})\rangle d\beta_{3\mu}. \qquad (3)$$

The coefficients $f(\beta_{3\mu})$ are determined by minimization of the total energy of the collective wave function $|\Psi\rangle$. In practice, the integral is replaced by a discrete summation over $\beta_{3\mu}$, with a number of points large enough to obtain results independent of the discretization[16,6]. The discretized Hill-Wheeler (HW) equation was solved separately for each collective coordinate Q_{30} and Q_{32}.

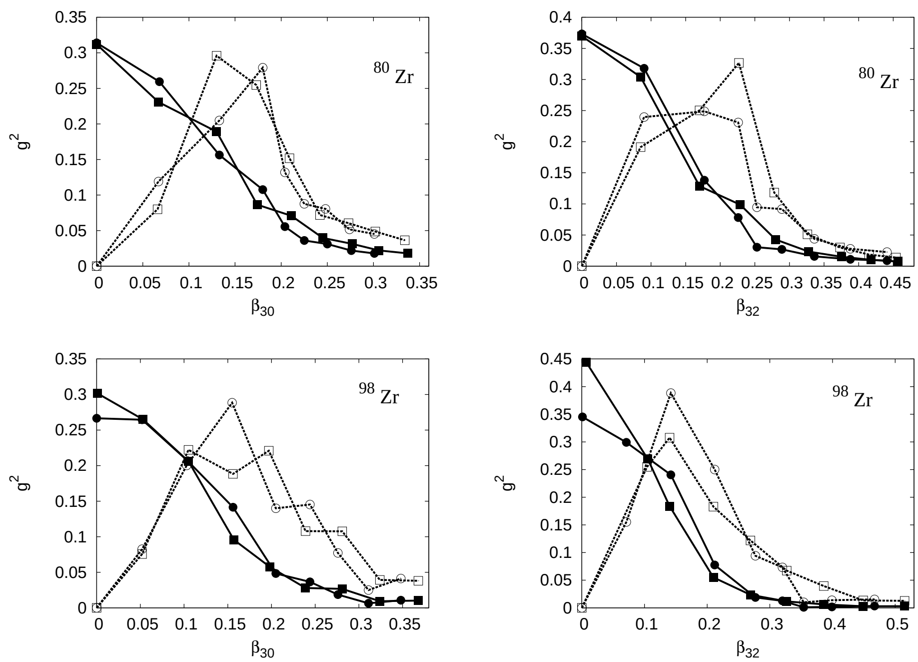

Fig. 4. The square of the modulus of the collective wave function vs. shape parameters are plotted for the Sly4 force. Two values of pairing strength have been considered: reproducing the experimental pairing gaps (circles) and with pairing gaps increased by a factor 2 (squares). The solid (dotted) lines with filled (open) symbols denote positive (negative) parity solutions.

In the Fig. 3 the collective wave functions (related to $f(\beta_{3\mu})$ by an integral transformation) are plotted for three parametrizations of the Skyrme force. One can see that all Skyrme forces give consistent results. The wave functions are spread around the minima of the projected mean-field energy curves, with a shape typical of a vibration in a 1-dimensional energy well. Note that there is no indication that any particular tetrahedral configuration contribute the most to the wave function. The large spread of the wave function confirms the importance of shape fluctuations. It is reflected also in the large value of the correlation energies which are listed in the table 1. Correlation energies have been calculated from the prescription:

$$E_{corr} = E(N, Z, spher.) - E^{+}, \tag{4}$$

where $E(N, Z, spher.)$ is the energy of the particle number projected spherical configuration obtained in the HFBCS approach, and E^{+} is the lowest positive-parity energy obtained in the GCM.

Note also that the collective wave functions for both axial octupole and tetrahedral coordinates have a very similar shape. Indeed the calculated correlation energies and excitation energies of the negative parity state have very similar values,

Table 1. Results of the GCM calculations for three Skyrme forces: SLy4, SIII and SkM*. $E_{corr}(Q_{\lambda\mu})$ represents the correlation energy associated with shape fluctuation described by $Q_{\lambda\mu}$ multipole moment (see eq. 4). Similarly $E_{exc}(Q_{\lambda\mu})$ denotes the excitation energy of the first negative-parity collective state with respect to the first positive-parity state. All values are in MeV.

Nucleus	SLy4	SIII	SkM*
^{80}Zr	$E_{corr}(Q_{30}) = 1.507$	1.459	1.290
	$E_{corr}(Q_{32}) = 1.567$	1.499	1.338
	$E_{exc}(Q_{30}) = 2.802$	2.520	3.111
	$E_{exc}(Q_{32}) = 2.425$	2.220	2.881
^{98}Zr	$E_{corr}(Q_{30}) = 1.389$	1.387	1.554
	$E_{corr}(Q_{32}) = 1.400$	1.485	1.564
	$E_{exc}(Q_{30}) = 2.644$	1.090	2.116
	$E_{exc}(Q_{32}) = 2.498$	0.784	1.776

slightly favoring the tetrahedral configuration.

In order to check the sensitivity of the GCM results on the magnitude of pairing correlations, we have performed calculations with pairing strengths that produce gaps larger or smaller by a factor 2. Qualitatively, the GCM results are not affected which can be seen in the Fig. 4. The correlation energies vary by $10 - 20\%$. A doubling of the pairing gap results in approximately twice larger excitation energy for the negative parity states.

4. Conclusions.

- The existence of a stable tetrahedral deformation at the mean-field level is rather unlikely for ^{80}Zr and ^{98}Zr.
- The parity projection induce a small tetrahedral (and also axial octupole) deformation which is relatively independent of the pairing strength.
- Shape fluctuations play an important role and significantly contribute to the correlation energy.
- Both axial octupole and tetrahedral states have very similar characteristics although the tetrahedral configuration is slightly more favored.

Summarizing we conclude that the existence of the tetrahedral deformation is of the dynamic character.

Acknowledgements

This work has been supported in part by the Polish Committee for Scientific Research (KBN) under Contract No. 1 P03B 059 27, the Foundation for Polish Science (FNP), the PAI-P5-07 of the Belgian Office for Scientific Policy. Numerical calculations were performed at the Interdisciplinary Centre for Mathematical and Computational Modelling (ICM) at Warsaw University.

References

1. I. Hamamoto, B. Mottelson, H. Xie, X. Z. Zhang, Z. Phys. **D21** (1991) 163.
2. X. Li and J. Dudek, Phys. Rev. **C49** (1994) R1250.
3. J. Dudek, A. Góźdź, N. Schunck, M. Miśkiewicz, Phys. Rev. Lett. **88** (2002) 252502. N. Schunck, J. Dudek, A. Góźdź and P.H. Regan, Phys. Rev. **C69** (2004) 061305(R).
4. J. Dudek, D. Curien, N. Dubray, J. Dobaczewski, V. Pangon, P. Olbratowski and N. Schunck, Phys. Rev. Lett. **97** (2006) 072501.
5. J. Dudek, A. Góźdź and N. Schunck, Acta Phys.Polon. **B34** (2003) 2491; N. Schunck, J. Dudek, Int. J. Mod. Phys. **E13** (2004) 213.
6. K. Zberecki, P. Magierski, P.-H. Heenen, N. Schunck, Phys. Rev. C (2006) *in press*, nucl-th/0604047.
7. P. Butler and W. Nazarewicz, Rev. Mod. Phys. **68** (1996) 349.
8. P. Bonche, H. Flocard and P.-H. Heenen, Comp. Phys. Comm. **171** (2005) 49.
9. P.-H. Heenen *et al.* Proc of Int. Workshop on Nuclear Structure Models, eds. R. Bengtsson, J. Draayer and W. Nazarewicz. (ORNL 1992), World Scientific (Singapore), p 3.
10. H.J. Lipkin, Ann. of Phys. **9** (1960) 272.
11. J. Dobaczewski, P. Magierski, W. Nazarewicz, W. Satuła and Z. Szymański, Phys. Rev. **C63** (2001) 024308.
12. M. Yamagami, K. Matsuyanagi, M. Matsuo, Nucl. Phys. **A693** (2001) 579.
13. S. Takami, K. Yabana, M. Matsuo, Phys. Lett. **B431** (1998) 242.
14. P. Olbratowski, J. Dobaczewski, P. Powałowski, M. Sadziak, K. Zberecki, Int. J. Mod. Phys. **E13** (2006) 333.
15. J. Skalski, P.-H. Heenen, P. Bonche, H. Flocard and J. Meyer, Nucl. Phys. **A551** (1993) 109.
16. M. Bender, P.-H. Heenen, and P.-G. Reinhard, Rev. Mod. Phys. **75** (2003) 121.